Desalination and Water Treatment
www.deswater.com
doi: 10.1080/19443994.2013.803696

52 (2014) 4273–4281
June

Taylor & Francis
Taylor & Francis Group

Removal of Ca(II) from aqueous solutions by cellulose modified with calix[4]arene

Yanmei Zhou*, Xiaoyi Hu, Min Zhang, Xiaofeng Zhuo

Institute of Environmental and Analytical Sciences, College of Chemistry and Chemical Engineering, Henan University, Kaifeng, Henan 475004, P.R. China
Tel. +86 378 2868633 3422; Fax: +86 378 3881589; email: zhouyanmei@henu.edu.cn

Received 11 June 2012; Accepted 23 April 2013

ABSTRACT

An adsorptive composite was prepared for calcium ions removal. The chemically modified cellulose (EMC) was grafted with the vinyl monomer glycidyl methacrylate using ceric ammonium nitrate as initiator and was further derived with calix[4]arene. The structure of the modified cellulose was characterized by using Fourier transform infrared (FTIR), scanning electron micrographs (SEM), thermogravimetric analysis (TGA), and X-ray diffraction (XRD). Epoxy cellulose was found to contain 3.17 mmol g^{-1} epoxy groups by the acetone-hydrochloride titration method. The adsorption process of EMC was described by the Langmuir model of adsorption well, and the maximum adsorption capacity of calcium ions reached 104.16 mg g^{-1}. The kinetic studies revealed that the adsorption process followed the pseudo-second-order kinetic model.

Keywords: Adsorption; Modified cellulose; Calcium ion; Calix[4]arene; Removal

---

1. Introduction

In order to remove the heavy metal ions, people usually add calcium oxide into the waste water. It could bring down the consistency of the heavy metals and turbidity of the water, but it will lead to the high content of calcium and hardness in water after the wastewater treatment. The higher hardness of the water induces scaling problems and serious failures in pipelines of boilers, heat exchangers, and electrical appliances such as washing machines, dishwashers, and steam irons [1,2]. Various methods have been available for the water softening such as chemical precipitation, ion exchanger process, nanofiltration, reverse osmosis and adsorption [3,4]. When compared to other methods, adsorption as a cost-effective and low-energy-consuming method, is gaining more and more attention.

Calixarenes are considered an important group of macrocycles as the third famous host molecules after cyclodextrins and crown ethers [5,6]. Calixarenes have generated considerable interest because of their property of the structure, which can selectively be functionalized at the lower (phenolic groups) or upper rim (aromatic nuclei) [7]. The calixarenes can be used in a variety after there are introduced various functional groups, such as analytical chemistry, membranes, catalysts, slow releasers of drugs, and decontaminating agents for wastewater [8–11]. Calixarene complexes with metal ions have been described in many times, and the number of report

---

*Corresponding author.

about this is enormous [12]. In the research of Farrokh, various types of calix[4]arene molecules were studied for complexation with alkali earth cations [13]. Zhang et al. synthesized the calixcrown could extract alkaline earth metal ions from aqueous solution into chloroform [14].

Cellulose, the most abundant biopolymer, has some prominent advantages such as low cost, biodegradability, good mechanical properties, nontoxicity, and high stability to most organic solvents [15]. Cellulose is a linear 1, 4-β-glucan polymer, compared with other polymers, the unit of the cellulose is very simple and uniform which make it formed highly ordered structures, and the three hydroxyl groups in each cellulose unit lead to extensive interaction through intra- and intermolecular hydrogen bonding [16]. Moreover, it has high density of hydroxyl groups on which different reactions can be carried out according to needs [17]. Recent investigation has shown that modified cellulose impressive removal efficiencies for the sorption of the metal ions from aqueous solutions. de Melo et al. modified cellulose with polysaccharide to removal cobalt and nickel [18]. Anirudhan et al. modified cellulose with tertiary amine functionality for the extraction of arsenic (V) [19]. Zhou et al. modified cellulose with β-CD, quaternary ammonium groups and D-Glucose to removal Cr(VI) from aqueous solutions [20,21].

In the existing literature, there are few literatures about the adsorption of Ca^{2+} and the capacities of the adsorption were not satisfactory. The aim of this study was to develop an economical, highly efficient and eco-friendly adsorbent. Taking all these prerequisites into consideration, we introduce the epoxy groups through graft the glycidyl methacrylate, and the calix[4]arene as functional group into the cellulose. In this work, we describe the design, synthesis, and the adsorption behavior of the chemically modified cellulose (EMC) (Fig. 1). The adsorption study was carried out to optimize various experimental parameters such as the effect of pH, contact time, temperature, and the calcium ion concentration. The kinetics and adsorption isotherm were investigated.

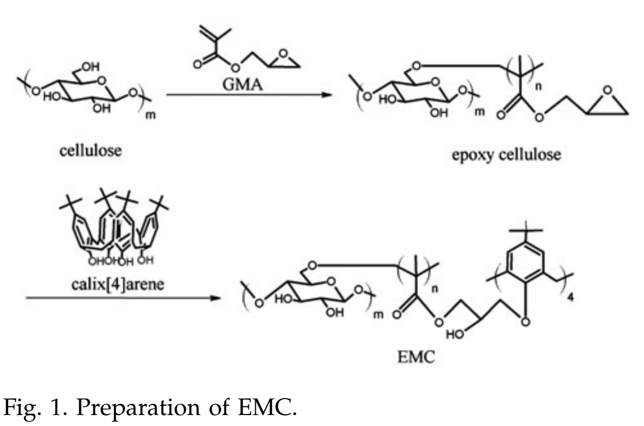

Fig. 1. Preparation of EMC.

2. Experiments

2.1. Materials and reagents

The cellulose was provided by Henan Xiren cellulose Co., Ltd. Glycidyl methacrylate (>99%, GMA) was obtained from Shangqiu Shengyuan Industrial Assistant Co. Ltd. Diphenyl ether and *p*-tert-butylphenol were purchased from Sinopharm Chemical Reagent Co. Ltd. All the other chemicals used in the experiment were purchased in analytical purity and were used without any purification. All aqueous solutions and standards were prepared using distilled water.

2.2. Preparation of EMC

The synthesis of the calix[4]arene using the *p*-tert-butylphenol and the formaldehyde according to the reported methods [22].

The cellulose was grafted with the vinyl monomer glycidyl methacrylate. In round flask, cellulose was initiated with $0.1\,\mathrm{mol\,L^{-1}}$ the ceric ammonium nitrate aqueous solution in water. The pH was adjusted to the range from 1.3 to 1.4 by hydrochloric acid. Then, GMA was added to the flask, the contents of the flask were heated for 2.5 h at 30°C under stirring in the N_2 atmosphere. The epoxy cellulose product was soxhlet extracted with acetone for 12 h to remove the GMA and then dried at 60°C under vacuum [23].

The epoxy cellulose was added to the flask and dispersed in DMF for 2 h. Then, sodium chloride solution ($0.5\,\mathrm{mol\,L^{-1}}$) and the calix[4]arene were added to the flask, and the mixture was heated at 70°C for 48 h. Filtration material that was washed with warm toluene, distilled water, acetone, and ethanol, respectively and then dried at room temperature. EMC was obtained.

2.3. Characterization of materials

2.3.1. Determination of the epoxy content in epoxy cellulose

The content of epoxy groups in the epoxy cellulose was determined by the acetone-hydrochloride titration method. The epoxy groups of epoxy cellulose reacted with HCl in acetone solution. The residual HCl was back-titrated with NaOH solution using phenolphthalein solution as indicator. The content of epoxy groups in the epoxy cellulose Epv (mmol g^{-1}) was expressed as follows:

$$Epv = \frac{(V_0 - V_1) \times C_{\mathrm{NaOH}}}{W_g} \tag{1}$$

where V_0 (mL) and V_1 (mL) are the titrimetric volume of NaOH by blank and sample consumed, respectively. C_{NaOH} (mol L^{-1}) is the amount of known NaOH molarity. W_g (g) is the weight of the epoxy cellulose.

2.3.2. FTIR characterization

Infrared spectra were measured on a Thermo Nicolet Avatar 360 FTIR Spectrometer in transmittance mode by the use of KBr pellets. Measurements were taken in the wavenumber range from 400 to 4,000 cm^{-1}.

2.3.3. Scanning electron microscopy characterization

Scanning electron micrographs of samples were recorded using a Jeol JSM5600LV scanning electron microscope.

2.3.4. Thermogravimetric and differential thermal analysis

Thermogravimetric analysis (TGA) and the differential thermal analysis (DTA) were acquired using Mettler-Toledo DTA/TGA instrument in the temperature range from 50 to 500°C at the rate of 10°C min^{-1} under nitrogen flow.

2.3.5. X-ray diffraction (XRD)

X-ray diffractograms were recorded using a X-Pert Pro X-ray diffractometer equipped with Cu K radiation at wavelength $\lambda = 0.15406$ nm, and the generator working at 40 kV and 40 mA. Diffractograms were collected in a 2θ range of 10–35° at the rate of 0.08°/s.

The crystallinity index (CrI) of cellulose samples was calculated from the XRD patterns by the following equation:

$$CrI = \frac{I_{200} - I_{am}}{I_{200}} \tag{2}$$

where I_{200} is the overall intensity of the peak at 2θ about 22°, and I_{am} is the intensity of the baseline at 2θ about 18°.

2.4. Batch adsorption experiments

Batch adsorption experiments were carried out by shaking 25 mg of EMC with 25 mL of a required metal ion concentration in different conical flasks using a temperature-controlled shaker. Then, the mixture was filtered out, and the filtrate was analyzed for the residual concentration.

The agitation speed was maintained at 180 rpm. The optimum pH, contact time, temperature, and the initial concentration were taken as the time at which maximum calcium ion took place.

The concentration of Ca^{2+} was determined by standard EDTA titration, eriochrome black T (EBT) as indicator and NH_3–NH_4Cl as buffer solution. The Ca^{2+} adsorption capacity of EMC was calculated as follows:

$$q = \frac{C_0 - C_t}{m} \times V \tag{3}$$

where q (mg g^{-1}) represents the amount of adsorbed cation, C_0 and C_t (mg L^{-1}) are the concentrations of adsorbed cation at initial and time t, respectively. V (L) is the volume of cation solution, and m (g) is the adsorbent mass.

3. Results and discussion

3.1. Structure characterization

3.1.1. Determination of the epoxy content in epoxy cellulose

As shown in Eq. (1), the epoxy groups content of the epoxy cellulose was calculated to contain 3.17 mmol g^{-1} by the acetone-hydrochloride titration method.

3.1.2. FTIR characterization

The Fourier transform infrared (FTIR) spectra of the cellulose, epoxy cellulose, and EMC are presented in Fig. 2. Fig. 2(A) shows the FTIR spectra in the wavenumber range from 400 to 4,000 cm^{-1}, and Fig. 2II shows the FTIR spectra in the wavenumber range from 500 to 2,000 cm^{-1}. In Fig. 2(B-b), the pronounced peaks of epoxy cellulose were shown at 756, 847, and 906 cm^{-1} were attributed due to the epoxy groups, and the peaks at 1,728 cm^{-1} was due to the C=O stretching, which can explained that the GMA has been grafted on the surface of the cellulose successfully. As shown in Fig. 2(B-b) and (B-c), the major change that can be found in FTIR spectrum for epoxy cellulose in relation to EMC is that the peaks at 756, 847, and 906 cm^{-1} of epoxy groups disappeared.

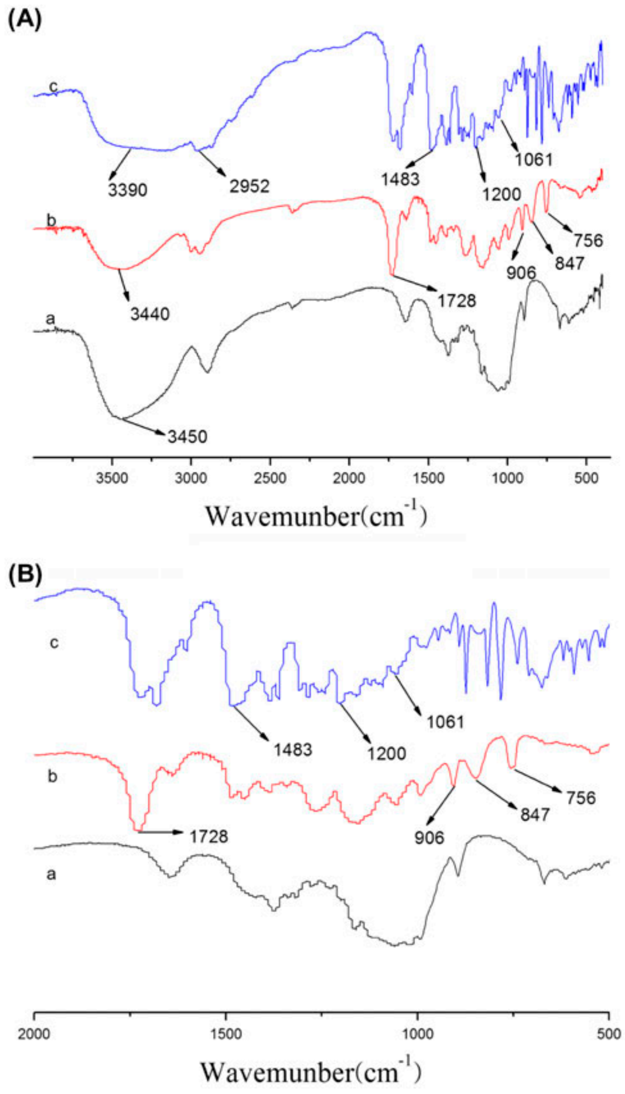

Fig. 2. FTIR of cellulose, epoxy cellulose, and EMC (a) cellulose; (b) epoxy cellulose; and (c) EMC.

In Fig. 2(A-c), the peaks at 1,061, 1,200, 1,483, and 2,952 cm^{-1} were due to the calix[4]arene, which can evidenced that the epoxy groups of the epoxy cellulose were reacted with calix[4]arene.

3.1.3. SEM characterization

Scanning electron micrographs (SEM) presented in Fig. 3 shows the surfaces of cellulose, epoxy cellulose, and EMC. It is observed that the surface of EMC have much more flakes, and rougher than that of cellulose and epoxy cellulose, which was due to the swelling effect of the cellulose and the surface of cellulose grafted GMA and calix[4]arene. The increases in the specific surface area provide proof of grafted and the changes positively affect the adsorption capacity.

3.1.4. TGA and DTA characterization

TGA and DTA curves for cellulose, epoxy cellulose, and EMC are presented in Fig. 4. The TGA curve of cellulose is characterized by one temperature zone. At the stage of decomposition ($T = 370^{\circ}$C), almost 90% is lost due to the decomposition of molecular compounds formed into large amounts of volatiles and solid char. The TGA and DTA curves of epoxy cellulose show the decomposition and weight loss at two different stages. The first stage comes between 190 and 245°C and the second between 245 and 425°C. The weight loss at the first stage ($T_1 = 230^{\circ}$C) is about 24% due to GMA polymer split from the cellulose and in the second stage decomposition ($T_2 = 360^{\circ}$C) of about 68% weight was lost leaving behind solid char. For EMC, the first stage of decomposition is in the range 159–213°C, the second is in the range 213–389°C, and the third is between 389 and 432°C [24]. The weight loss at the first-stage ($T_1 = 131^{\circ}$C) is due to the pyrolytic decomposition of calix[4]arene, in the second-stage decomposition ($T_2 = 210^{\circ}$C) about 77% weight was lost, and the third-stage decomposition ($T_3 = 347^{\circ}$C) of about 9% weight was lost due to the thermal cleavage of the glucosidic units and scission of the C–O bonds [25].

3.1.5. X-ray diffraction characterization

The X-ray diffraction (XRD) patterns of the cellulose and EMC are presented in Fig. 5. The cellulose with diffraction peaks at 15.2°, 16.7°, 22.9°, and 34.4° shows the characteristic crystalline form of cellulose with crystalline index (CrI) of 74.19%. Compared to the cellulose, the diffractions of EMC at 2θ of 13.8°, 20.6°, 25.7°, and 28.4° were observed, which can be assigned to the typical diffractions of EMC with CrI of 50.12% that shows the crystalline transformation of cellulose occurred during the reaction. Compare with the cellulose, the peak intensity and CrI of the EMC obviously decreased, this may be due to the introduction of the grafted chain, which changes the aggregation structure of the cellulose, destroyed the highly ordered and crystalline regions [26]. And prolonged exposure to acid condition, which can reduce crystallinity as the crystalline regions are increasingly subject to hydrolysis [27,28].

3.2. Effect of pH on Ca^{2+} adsorption

The solution pH is generally known to play a very important role in adsorption process presumably due to its influence on the surface properties of the adsorbent and ionization/dissociation of the adsorbate

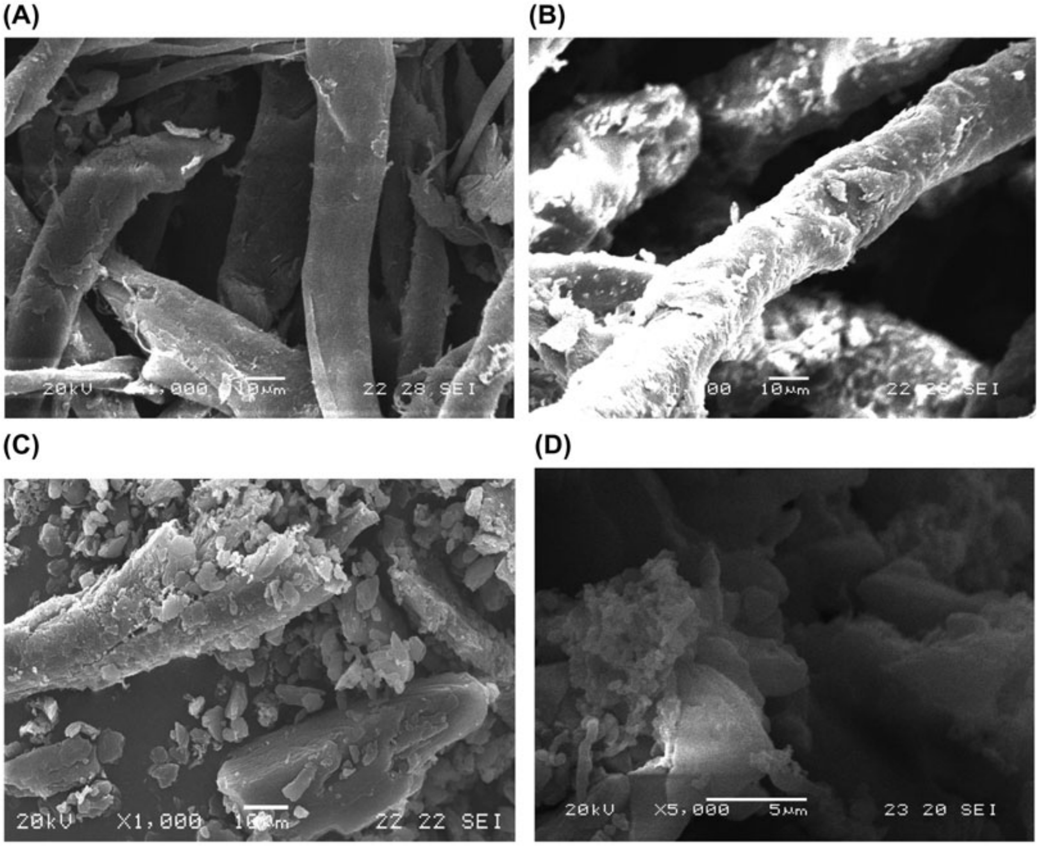

Fig. 3. SEM morphology of cellulose, epoxy cellulose, and EMC (A) Cellulose magnification 1,000×; (B) Epoxy cellulose magnification 1,000×; (C) EMC magnification 1,000×; and (D) EMC magnification 5,000×.

molecule [29]. The effect of pH on the adsorption of Ca^{2+} by EMC was studied by varying the pH from 3.0 to 9.0 for an initial Ca^{2+} concentration of $400\,mg\,L^{-1}$, and the results are shown in Fig. 6. The adsorption capacity was found to increase with increase in pH up to a maximum at pH 7.0 and after that it showed a decrease. This could be explained as follows: at low pH, the high concentration of hydronium ions (H_3O^+) restrict the metal cations approach with the functional groups of EMC, because of the repulsive force [30]. With the pH increasing, more functional groups join in metal ion uptake, the adsorption capacity increases. But at the high pH value, adsorption was reduced because the competitive adsorption of hydroxyl reacted with the Ca^{2+} ions. So the pH 7.0 was selected as the optimum pH of all subsequent adsorption experiments.

3.3. Effect of the temperature on Ca^{2+} adsorption

As shown in Fig. 7, the effect of the temperature on adsorption of Ca^{2+} was studied by varying the temperature from 15 to 55°C. The adsorption capacity was found to increase with the change of the temperature from 15 to 35°C, and it showed indistinctive after 35°C. Therefore, the temperature of 35°C was used in the subsequent studies.

3.4. Effect of contact time on Ca^{2+} adsorption

Adsorption time was investigated to determine adsorption equilibrium time for EMC. The effect of contact time on the adsorption was shown in Fig. 8. It was found that the initial portion of adsorption capacity increased quickly, and the equilibrium was attained in 1 h. So it was selected as the optimum contact time.

3.5. Kinetic study

The kinetics of adsorption is desirable, as it was used to evaluate the mechanism of adsorption, which is important for optimizing the efficiency of the adsorption process [29]. Adsorption kinetics of Ca^{2+} onto EMC was studied using pseudo-first-order Eq. (4) and pseudo-second-order kinetic model Eq. (6), the

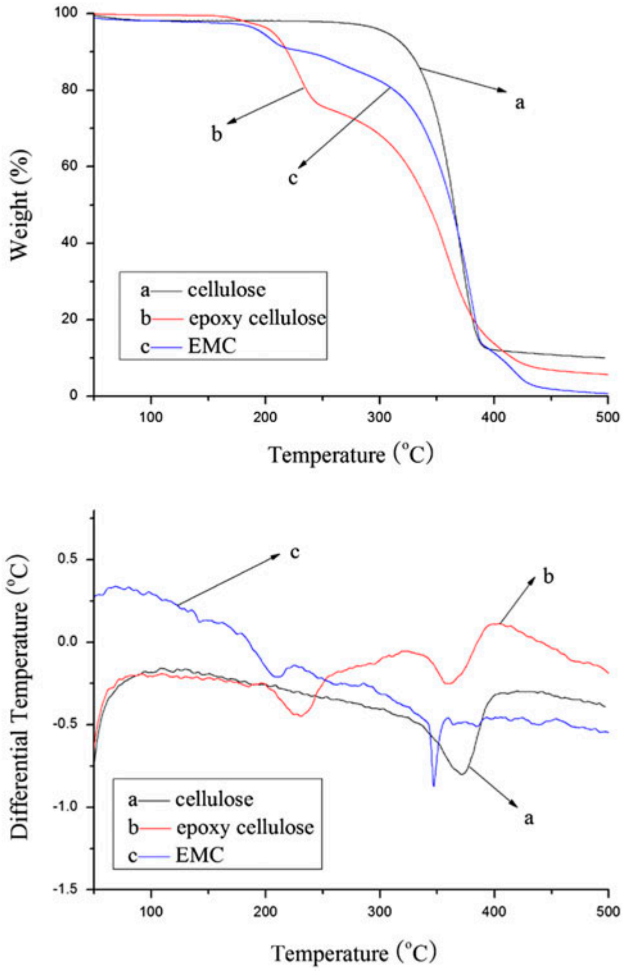

Fig. 4. TGA and DTA curves of cellulose, epoxy cellulose and EMC.

pseudo-first-order model and the pseudo-second-order model can be represented in linear form Eqs. (5) and (7), respectively [31]. The fit quality was measured through coefficient of determination (R^2) and average relative error (ARE).

$$q_t = q_e(1 - e^{-k_1 t}) \tag{4}$$

$$\ln(q_e - q_t) = \ln q_e - k_1 t \tag{5}$$

$$q_t = \frac{k_2 q_e^2 t}{1 + k_2 q_e t} \tag{6}$$

$$\frac{t}{q_t} = \frac{1}{k_2 q_e^2} + \frac{t}{q_e} \tag{7}$$

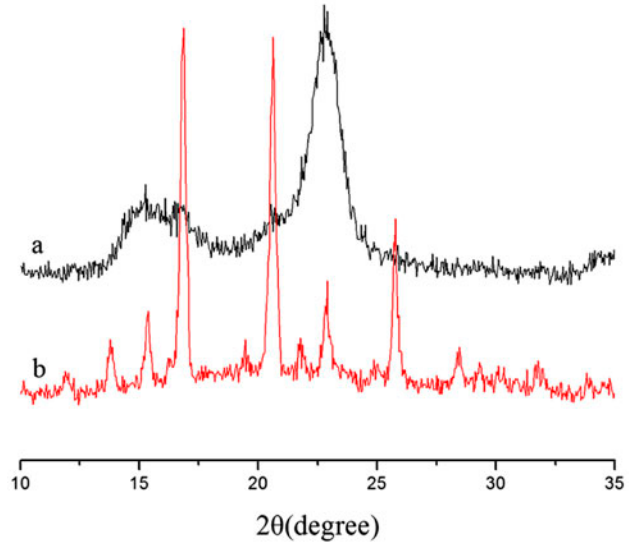

Fig. 5. XRD patterns for cellulose and EMC (a) cellulose; and (b) EMC.

where q_e (mg g^{-1}) and q_t (mg g^{-1}) are the amounts of solute adsorbed per unit mass of the adsorbent at equilibrium and time t, respectively. k_1 (g mg^{-1} min^{-1}) and k_2 (dm^3 mg^{-1} min^{-1}) are the pseudo-first-order and pseudo-second-order rate constants, respectively. The pseudo-first-order and pseudo-second-order models describe the kinetics of the solid-solution system based on mononuclear and binuclear adsorption, respectively, with respect to the sorbent capacity [32]. We can obtain some results by analyzing Fig. 8, and parameter listed in Table 1. The pseudo-first-order equation shows a poor correlation with experimental

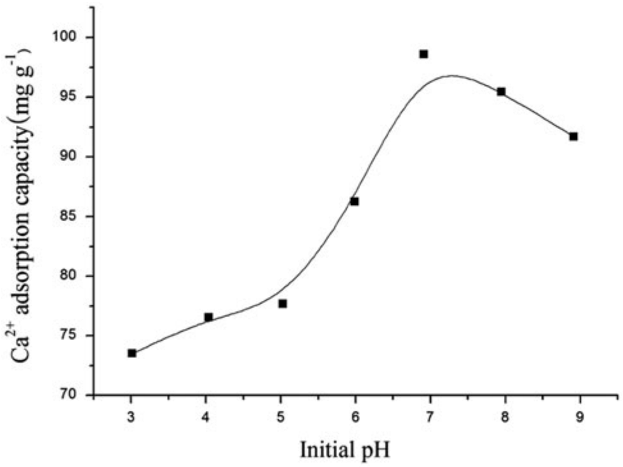

Fig. 6. Effect of pH on Ca^{2+} adsorption. Conditions: 400 mg L^{-1} Ca^{2+} solution; temperature, 35°C; contact time, 120 min; adsorbent, 25 mg.

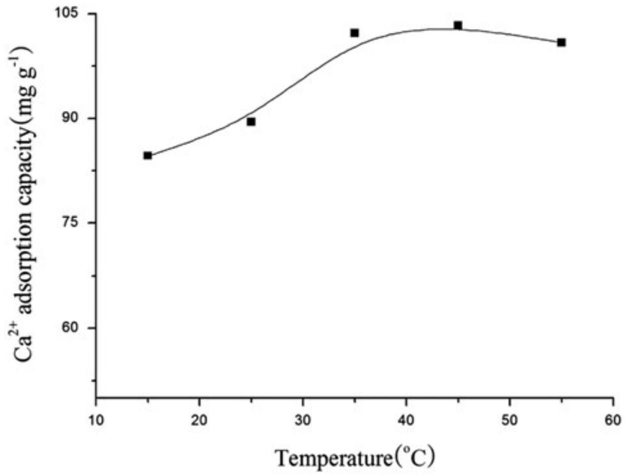

Fig. 7. Effect of the temperature on Ca^{2+} adsorption. Conditions: 400 mg L^{-1} Ca^{2+} solution; pH, 7.0; contact time, 120 min; adsorbent, 25 mg.

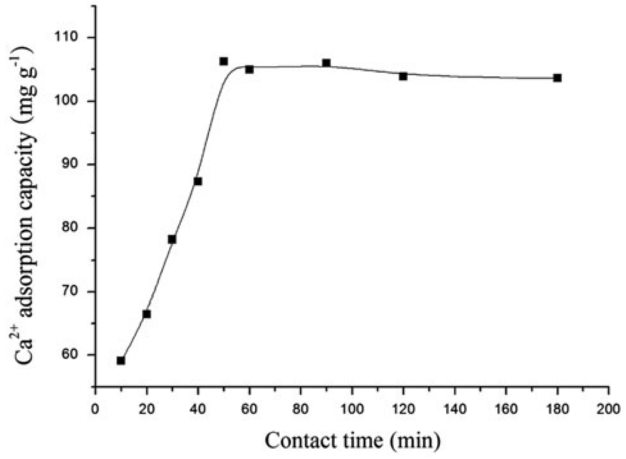

Fig. 8. Effect of contact time on Ca^{2+} adsorption. Conditions: 400 mg L^{-1} Ca^{2+} solution; pH, 7.0; temperature, 35°C; adsorbent, 25 mg.

data, whereas the pseudo-second-order equation indicates a good correlation of the experimental results. So the kinetics of Ca^{2+} adsorption on EMC accords with the pseudo-second-order kinetic process correctly.

3.6. Adsorption isotherms

Adsorption isotherms are used to describe how solutes interact with adsorbent and determine the maximum adsorption capacity of the adsorbent [33]. The equilibrium sorption isotherms were analyzed by the two most commonly used model equations, which were Langmuir and Freundlich.

The Langmuir isotherm assumes monolayer coverage of adsorbate over a homogeneous adsorbent surface, and the adsorption of each molecule on the surface has equal adsorption activation energy. Langmuir equation can be expressed as follows:

$$q_e = \frac{Q^0 k_L C_e}{1 + k_L C_e} \tag{8}$$

$$\frac{C_e}{q_e} = \frac{C_e}{Q^0} + \frac{1}{Q^0 k_L} \tag{9}$$

where C_e (mg L^{-1}) and q_e (mg g^{-1}) are the concentration and adsorption capacity at the equilibrium, respectively. Q^0 (mg g^{-1}) and k_L (L mg^{-1}) are adsorption capacity and binding energy of adsorption of Langmuir, respectively.

Freundlich isotherm supposes a heterogeneous surface with a nonuniform distribution of heat of adsorption over the surface and a multilayer adsorption can be expressed. The Freundlich equation can be expressed as follows:

$$q_e = K_F C_e^{\frac{1}{n_F}} \tag{10}$$

$$\ln q_e = \ln K_F + \frac{1}{n_F} \ln C_e \tag{11}$$

where C_e (mg L^{-1}) and q_e (mg g^{-1}) are the concentration and adsorption capacity at the equilibrium, respectively. K_F and n_F are Freundlich constants measuring the adsorption capacity and the adsorption intensity, respectively.

The Langmuir and Freundlich isotherm parameters were determined using linear regression analysis, and

Table 1
Pseudo-first-order and pseudo-second-order models for the adsorption of Ca^{2+} onto EMC

Kinetics models	Parameters				
	q_e (mg g^{-1})	k_1 (g mg^{-1} min^{-1})	k_2 (g mg^{-1} min^{-1})	R^2	ARE (%)
Pseudo-first-order	105.99	7.68×10^{-2}	–	0.7353	1.73
Pseudo-second-order	106.61	–	2.52×10^{-3}	0.9973	2.30

Conditions: 0.01 mol L^{-1} Ca^{2+} solution; pH, 7.0; temperature, 35°C; adsorbent, 25 mg.

Table 2
Langmuir and Freundlich isotherm models for adsorption of Ca^{2+} onto EMC

Isotherm models	Parameters				
	k_L (L mg^{-1})	K_F (L g^{-1})	Q^0 (mg g^{-1})	n_F	R^2
Langmuir	5.34×10^{-2}	–	104.16	–	0.9974
Freundlich	–	87.47	–	30.3	0.9196

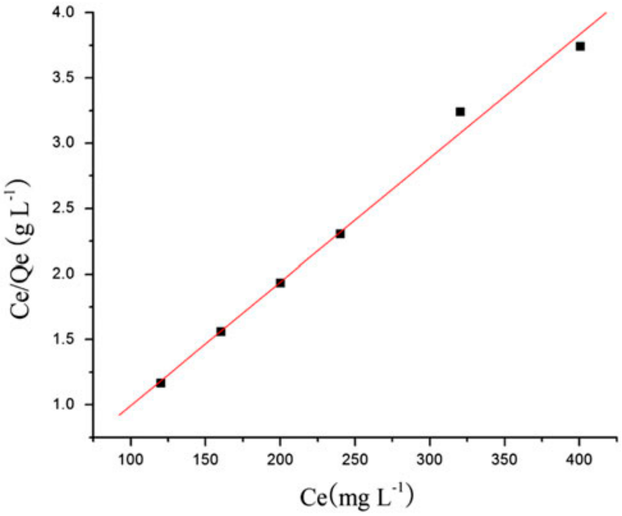

Fig. 9. Langmuir isotherm for Ca^{2+} adsorption on EMC. Condition: pH, 7.0; temperature, 35°C; contact time, 60 min; adsorbent, 25 mg.

the values are listed in Table 2. As can be seen from the results, equilibrium data agree well with the Langmuir model. The value of the correlation coefficient (R^2) showed that the adsorption of Ca^{2+} onto EMC was best fitted with Langmuir isotherm model over the concentration ranges studied. The constants of Langmuir isotherm model were calculated by Fig. 9. Q^0 was calculated to be 104.16 mg g^{-1}.

4. Conclusions

A novel adsorbent EMC, which was grafted GMA and calix[4]arene on the cellulose structure, was synthesized, characterized and its efficiency in uptake Ca^{2+} was tested by batch adsorption technique, the effects of adsorption conditions on adsorptive performance were investigated. The adsorption process, which was pH dependent, shows maximum removal at pH 7.0. Adsorption equilibrium was achieved within 60 min. The adsorption process fit the Langmuir isotherm and the pseudo-second-order kinetics model. Based on the above results, the EMC adsorbent can be used as one of efficient adsorbents to treat with calcium ions from the aqueous solution.

Acknowledgements

The authors are grateful for the key scientific and technological project of Henan province (112102310360, 122300410260), the natural science research project of Henan province education department (2011A610005) and the financial support of the foundation of International scientific and technological cooperation of Henan province (124300510012) in China. The authors also thank the anonymous reviewers for their invaluable insight and helpful suggestions.

References

[1] C. Gabrielli, G. Maurin, H. Francy-Chansson, P. Thery, T.T.M. Tran, M. Tlili, Electrochemical water softening: Principle and application, Desalination 201 (2006) 150–163.
[2] O.K. Júnior, L.V.A. Gurgel, L.F. Gil, Removal of Ca(II) and Mg(II) from aqueous single metal solutions by mercerized cellulose and mercerized sugarcane bagasse grafted with EDTA dianhydride(EDTAD), Carbohyd. Polym. 79 (2010) 184–191.
[3] S.J. Seo, H. Jeon, J.K. Lee, G.Y. Kim, D. Park, H. Nojima, J. Lee, S.H. Moon, Investigation on removal of hardness ions by capacitive deionization (CDI) for water softening applications, Water Res. 44 (2010) 2267–2275.
[4] D. Nemeth, J. Labidi, L. Gubicza, K. Belafi-Bako, Comparative study on heavy metal removal from industrial effluents by various separation methods, Desalin. Water Treat. 35 (2011) 242–246.
[5] B. Mokhtari, K. Pourabdollah, N. Dalali, Analytical applications of calixarenes from 2005 up-to-date, J. Incl. Phenom. Macro. 69(2011) (2005) 1–55.
[6] M.A. Kamboh, I.B. Solangi, S.T.H. Sherazi, S. Memon, A highly efficient calix[4]arene based resin for the removal of azo dyes, Desalination 268 (2011) 83–89.
[7] A.R. Hajipour, S. Habibi, A.E. Ruoho, Modification of poly acrylic acid using calix[4]arene derivative for the adsorption of toxic heavy metals, J. Appl. Polym. Sci. 118 (2010) 818–826.
[8] F. Gharib, M. Hajmalek, R.A. Alamoti, A. Farajtabar, Complexation of dioxovanadium (V) and dioxouranium (VI) by *p*-sulphonato-calix[4]arene in aqueous solution, J. Mol. Liq. 159 (2011) 161–164.
[9] Y. Koide, H. Sato, H. Shosenji, K. Yamada, Emulsification of calix[4]arenes bearing four chains and transportation of cesium ion through liquid surfactant-membrane, B. Chem. Soc. Jpn. 69 (1996) 315–319.
[10] T. Jin, M. Kinjo, T. Koyama, Y. Kobayashi, H. Hirata, Selective Na^+ transport through phospholipid bilayer membrane by a synthetic calix[4]arene carrier, Langmuir 12 (1996) 2684–2689.
[11] B. Nilius, J. Prenen, G. Droogmans, Modulation of volume-regulated anion channels by extra- and intracellular pH, Pflügers Arch.-Eur. J. Physiol. 436 (1998) 742–748.

[12] W. Sliwa, T. Girek, Calixarene complexes with metal ions, J. Incl. Phenom. Macro. 66 (2010) 15–41.

[13] G. Farrokh, T. Saeid, G. Sara, Complexation of di-benzyloxy ether derivatives of calix[4]arene with alkali earth metal cations, Russ. J. Inorg. Chem. 52 (2007) 1915–1917.

[14] D.M. Zhang, X.D. Cao, D.W. Purkiss, R.A. Bartsch, Di-ionizable p-tert-butylcalix[4]arene-1,2-crown-3 ligands in cone and 1,2-alternate conformations: Synthesis and metal ion extraction, Org. Biomol. Chem. 5 (2007) 1251–1259.

[15] S.L. Chen, X.J. Huang, Z.K. Xu, Functionalization of cellulose nanofiber mats with phthalocyanine for decoloration of reactive dye wastewater, Cellulose 18 (2011) 1295–1303.

[16] P. Goswami, R.S. Blackburn, J. Taylor, P. White, Sorption of dyes on cellulose II: Effect of alkali treatment of fibre and dye structure, Cellulose 18 (2011) 1063–1072.

[17] J.K. Pandey, C.S. Lee, S.H. Ahn, Preparation and properties of bio-nanoreinforced composites from biodegradable polymer matrix and cellulose whiskers, J. Appl. Polym. Sci. 115 (2010) 2493–2501.

[18] J.C.P. de Melo, E.C. da Silva Filho, S.A.A. Santana, C. Airoldi, Exploring the favorable ion-exchange ability of phthalylated cellulose biopolymer using thermodynamic data, Carbohyd. Polym. 345 (2010) 1914–1921.

[19] T.S. Anirudhan, S. Jalajamony, Cellulose-based anion exchanger with tertiary amine functionality for the extraction of arsenic (V) from aqueous media, J. Environ. Manage. 91 (2010) 2201–2207.

[20] Y.M. Zhou, Q. Jin, T.W. Zhu, Y. Akama, Adsorption of chromium (VI) from aqueous solution by cellulose modified with β-CD and quaternary ammonium groups, J. Hazard. Mater. 187 (2011) 303–310.

[21] Y.M. Zhou, Q. Jin, T.W. Zhu, T.S. Ma, X.Y. Hu, Removal of chromium (VI) from aqueous solution by cellulose modified with D-glucose, Sep. Sci. Technol. 47 (2012) 157–165.

[22] C.D. Gutsche, M. Iqbal, P-tert-butylcalix[4]arene, Organic Synth. 68 (1990) 234–238.

[23] R.R. Navarro, K. Sumi, M. Matsumura, Improved metal affinity of chelating adsorbents through graft polymerization, Water Res. 33 (1999) 2037–2044.

[24] S.R. Shukla, A.R. Athalye, Mechanical and thermal properties of glycidyl methacrylate grafted cotton cellulose, J. Appl. Polym. Sci. 57 (1995) 983–988.

[25] M. Huang, X. Li, Thermal degradation of cellulose and cellulose esters, J. Appl. Polym. Sci. 68 (1998) 293–304.

[26] R. Krishnaveni, S. Thambidurai, Effect of solvents on cyanoethylation of cotton cellulose and its properties, J. Appl. Polym. Sci. 122 (2011) 1622–1627.

[27] L.R. Tang, B. Huang, W. Ou, X.R. Chen, Y.D. Chen, Manufacture of cellulose nanocrystals by cation exchange resin-catalyzed hydrolysis of cellulose, Biores. Technol. 102 (2011) 10973–10977.

[28] J. Geboers, S.V. de Vyver, K. Carpentier, P. Jacobs, B. Sels, Efficient hydrolytic hydrogenation of cellulose in the presence of Ru-loaded zeolites and trace amounts of mineral acid, Chem. Commun. 47 (2011) 5590–5592.

[29] P. Vijayalakshmi, V.S.S. Bala, K.V. Thiruvengadaravi, P. Panneerselvam, M. Palanichamy, S. Sivanesan, Removal of acid violet 17 from aqueous solutions by adsorption onto activated carbon prepared from pistachio nut shell, Sep. Sci. Technol. 46 (2011) 155–163.

[30] L.V.A. Gurgel, L.F. Gil, Adsorption of Cu (II), Cd (II) and Pb (II) from aqueous single metal solutions by succinylated twice-mercerized sugarcane bagasse functionalized with triethylenetetramine, Water Res. 43 (2009) 4479–4488.

[31] H.H. Gan, G.K. Zhang, Y.L. Zhang, Y.D. Guo, Adsorption of rhodamine B from aqueous solution onto sepiolite modified by cetyltrimethylammonium bromide, Desalin. Water Treat. 45 (2012) 112–119.

[32] C. Gerente, V.K.C. Lee, P. Le Cloirec, G. McKay, Application of chitosan for the removal of metals from wastewaters by adsorption-mechanisms and models review, Crit. Rev. Environ. Sci. Technol. 37 (2007) 41–127.

[33] T.S. Anirudhan, P. Senan, P.S. Suchithra, Evaluation of iron (III)-coordinated amino-functionalized poly(glycidyl methacrylate)-grafted cellulose for arsenic(V) adsorption from aqueous solutions, Water Air Soil Pollut. 220 (2011) 101–116.